Eurographics Workshop on Visual Computing for Biology and Medicine (2015)
K. Bühler, L. Linsen, and N. W. John (Editors)

Simulated Motion Artefact in Computed Tomography

F. P. Vidal[1,2] and P.-F. Villard[3]

[1]School of Computer Science, Bangor University, LL57 1UT, United Kingdom
[2]Research Institute of Visual Computing, RIVIC
[3]LORIA, University of Lorraine, France

Abstract

We propose a simulation framework to simulate the computed tomography acquisition process. It includes five components: anatomic data, respiration modelling, automatic parametrisation, X-ray simulation, and tomography reconstruction. It is used to generate motion artefacts in reconstructed CT volumes. Our framework can be used to evaluate CT reconstruction algorithm with motion artefact correction in a controlled environment.

Categories and Subject Descriptors (according to ACM CCS): I.3.8 [Computer Graphics]: Applications—Medical I.3.5 [Computer Graphics]: Computational Geometry and Object Modeling—I.6.3 [Simulation and Modeling]: Applications—Medical

1. Introduction

In this paper we combine to simulation tools together to simulate the tomography acquisition process:

- Anatomical structures are animated with a visually realistic respiration model.
- This virtual physiological human (VPH) is placed in a virtual CT scanner using X-ray simulation.

Many X-ray projections at successive angles around the patient is then computed. It produces a sinogram, which is the input data of reconstruction algorithms that create CT slices. Our aim is to simulate data that will generate realistic motion artefacts in CT images.

2. Respiration Modelling

Anatomical data from 4D CT scans is segmented to provide polygon meshes. The motion due to the respiration is computed in realtime using three different methods [VVH*09]. The rib cage motion is simulated by an articulated model of the rib rotations. The diaphragm behaviour is simulated by a deformable model with an intrinsic force to apply contraction and relaxation on its central tendon. The liver behaviour is simulated by a deformable model where boundary conditions are applied by both the rib cage and the diaphragm motion. The 3D Chainmail method is used to deform soft-tissues in real-time [LB03]. The model includes many parameters, which are automatically tuned using artificial evolution [VVL12].

3. X-ray Simulation

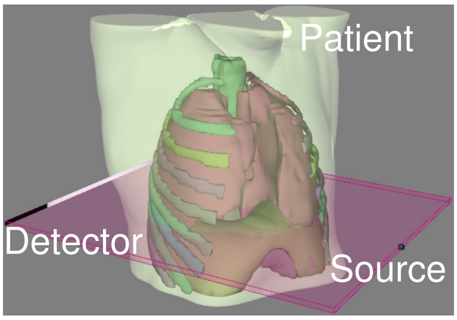

Figure 1: *Scanning environment.*

In [VGF*09] we proposed a method to compute the X-ray attenuation law on the GPU. The code has been revised and a quantitative validation has been performed. It shows the accuracy of results produced with our implementation. The result is *gVirtualXRay, Virtual X-Ray Imaging Library on GPU*, an OpenSource Library available at `http://gvirtualxray.sourceforge.net/`.

Fig. 1 shows the virtual scanning environment. The

DOI: 10.2312/vcbm.20151228

geometry of the virtual patient is positioned in the centre of the CT scanner. For each anatomical structure (skin, liver, diaphragm, lungs, ribs, and spine), a Hounsfield value is associated to a polygon mesh. The CT scanner is made of a rotation axis, a parallel X-ray source, and a detector. The source and detector rotate around the patient. The source can be monochromatic or polychromatic and it has an initial position. The detector is defined by its initial position and its size (number of pixels and pixel resolution).

4. CT Acquisition

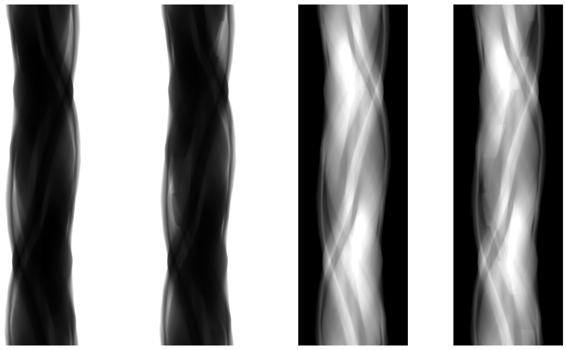

(a) (b) (c) (d)

Figure 2: *Simulated CT data acquisition; (a) & (b) X-ray projections; (a) without respiration; (b) with respiration; (c) & (d) corresponding sinograms.*

The respiration frequency of the patient and angular frequency of the source/detector couple can be tuned. In the illustrations, we use realistic parameters: 20 breaths per minutes and 15 second to perform a complete circular revolution. Successive projections are then concatenated and finally transformed into a sinogram (i.e. a Radon transform) (see Fig. 2).

5. CT Reconstruction

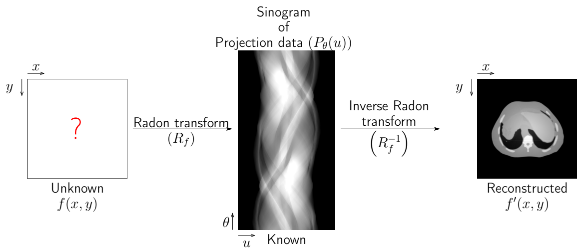

Figure 3: *CT reconstruction principle.*

To reconstruct a CT slice, the inverse Radon transform of the sinogram needs to be computed (see Fig. 3). We use the famous filtered back projection (FBP) method. No motion artefact can be seen in the CT slice corresponding to the sinogram simulated without respiration (see Fig. 4(a)). When respiration is used, ghost artefacts can be seen (see Fig. 4(b)).

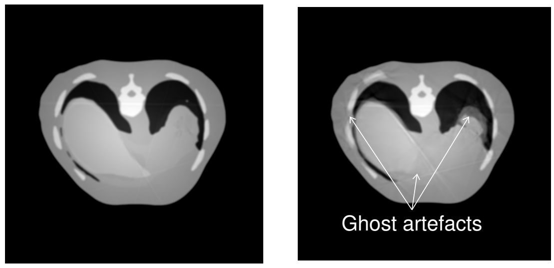

(a) Without respiration. (b) With respiration.

Figure 4: *Reconstructed CT slices.*

6. Conclusions

This poster focused on the simulation of CT data acquisition with respiration modelling. It involves two simulation components: Respiration and X-ray. Both run with real-time performance. Slices reconstructed with the resulting data include ghosting artefacts due to motion. We demonstrated that realistic data can now be simulated in a controlled environment. Our framework can be used to evaluate motion correction methods in CT reconstruction algorithms.

Acknowledgements

This work has been partially funded by FP7-PEOPLE-2012-CIG project Fly4PET – Fly Algorithm in PET Reconstruction for Radiotherapy Treatment Planning (`http://fly4pet.fpvidal.net`).

References

[LB03] Li Y., Brodlie K.: Soft Object Modelling with Generalised ChainMail - Extending the Boundaries of Web-based Graphics. *Comput Graph Forum 22*, 4 (2003), 717–727. doi:10.1111/j.1467-8659.2003.00719.x. 1

[VGF*09] Vidal F. P., Garnier M., Freud N., Létang J. M., John N. W.: Simulation of X-ray attenuation on the GPU. In *Proc Theor Pract Comput Graph* (2009), Eurographics Association, pp. 25–32. doi:10.2312/LocalChapterEvents/TPCG/TPCG09/025-032. 1

[VVH*09] Villard P., Vidal F. P., Hunt C., Bello F., John N. W., Johnson S., Gould D. A.: Simulation of percutaneous transhepatic cholangiography training simulator with real-time breathing motion. *Int J Comput Assist Radiol Surg 4*, 9 (2009), 571–578. doi:10.1007/s11548-009-0367-1. 1

[VVL12] Vidal F. P., Villard P., Lutton E.: Tuning of patient specific deformable models using an adaptive evolutionary optimization strategy. *IEEE IEEE Trans Biomed Eng 59*, 10 (2012), 2942–2949. doi:10.1109/TBME.2012.2213251. 1